Conventional and density-fitting local Møller–Plesset theory calculations of C_{60} and its endohedral $H_2@C_{60}$ and $2H_2@C_{60}$ complexes

Grygoriy A. Dolgonos [a,*], Gilles H. Peslherbe [b]

[a] Bremen Center for Computational Materials Science (BCCMS), University of Bremen, Am Fallturm 1, 28359 Bremen, Germany
[b] Centre for Research in Molecular Modeling (CERMM) and Department of Chemistry & Biochemistry, Concordia University, 7141 Sherbrooke St. West, Montréal, QC, Canada H4B1R6

ARTICLE INFO

ABSTRACT

The geometries of C_{60} and the $H_2@C_{60}$ and $2H_2@C_{60}$ complexes have been fully optimized at the density-fitting local second-order Møller–Plesset (DF-LMP2) level of theory and compared to their conventional MP2 counterparts. A slight elongation of the H—H bond is found in $H_2@C_{60}$, which leads to a red shift of the H—H vibrational frequency, relative to that of free H_2, consistent with reported experimental data. The $2H_2@C_{60}$ is characterized by a slight cage expansion and a blue C—C vibrational frequency shift. The DF-LMP2/cc-pVTZ complexation energies are equal to -5.6 and $+3.0$ kcal/mol, for one and two encapsulated H_2 molecules, respectively, and agree well with former theoretical estimates.

1. Introduction

Hydrogen storage in fullerenes by means of endohedral complex formation with H_2 molecules has been a subject of controversy among computational physicists and chemists as the predicted stability of $nH_2@C_n$ complexes strongly depends on the computational method employed. In the case of $H_2@C_{60}$, one would *a priori* expect a moderately stable complex, due to the nonbonding interactions between the hydrogen and carbon atoms, whereas with more hydrogen molecules inserted, the $nH_2@C_{60}$ complexes become thermodynamically unstable [1–3]. However, most of the low-level quantum chemistry approaches such as Hartree–Fock theory, semiempirical methods and standard density-functional theory (DFT) fail to properly describe weakly bound systems [4], for which van der Waals interactions play a significant role in the complex formation [5–7]. It should be noted that recent DFT functionals of meta-GGA [8–11] or double-hybrid [12] type may yield the proper stability trends, but their performance still needs to be thoroughly tested with respect to basis set size and the corresponding basis set superposition errors (see, for instance, Ref. [13]). Alternatively, the dispersion-corrected DFT-D [14] approach (in particular, its most advanced version, DFT-D3 [15]) could be used to account for long-range correlation effects and to describe nonbonded systems properly.

More sophisticated and computationally demanding quantum chemistry methods that take into account electron correlation are still impractical in fullerene research since their scaling of computational cost with respect to basis set size is too steep. Nevertheless,

recent developments in reduced-scaling approaches (see Ref. [16] and references therein), including local (L) correlation methods based on Pulay's localized molecular orbitals [17–19], as well as density-fitting (DF) – also sometimes referred to as 'resolution of the identity' (RI) – approximations for the evaluation of integrals [20,21], lead to a speedup of 1–2 orders of magnitude, and to a linear scaling of computational cost, while retaining the accuracy of the conventional methods. For instance, the potential energy curves of different benzene dimer conformers computed with the density-fitting local second-order Møller–Plesset theory (DF-LMP2 [21]) almost coincide with those calculated using counterpoise-corrected [22] conventional second-order Møller–Plesset theory (MP2 [23]) [24]. This suggests that DF-LMP2 calculations for $nH_2@C_{60}$ complexes, whose stability is mainly due to London dispersion interactions and which require a proper treatment of electron correlation, should also yield results of MP2 quality.

A few attempts have been reported in the literature to apply MP2, RI-MP2 and symmetry-adapted perturbation theory (SAPT) to endohedral complexes of hydrogen molecules in C_{60} and C_{70} [3,25–28]. Because of the high computational cost, energy calculations have been performed for these systems up to now based on either experimental C_{60} and H_2 geometries [3,28] or for optimized geometries determined by DFT [25,26] or Hartree–Fock [27] calculations. Therefore, the influence of full geometry relaxation on the complexation energies has not been addressed in the literature so far. In addition, the use of small basis sets in conjunction with MP2 may lead to a relatively large basis set superposition error (BSSE), which must be taken into account in order to avoid a significant overestimation of the $nH_2@C_{60}$ complex stability.

In this Letter, we analyze the influence of full geometry relaxation and BSSE on the complexation energies of $H_2@C_{60}$ and $2H_2@C_{60}$,

* Corresponding author. Fax: +49 (0)421 218 4764.
E-mail addresses: grygoriy.dolgonos@bccms.uni-bremen.de, dolgonos@gmail.com (G.A. Dolgonos).

based on conventional MP2 and DF-LMP2 calculations with double- and triple-zeta basis sets.

2. Computational methodology

The structures of C_{60}, $H_2@C_{60}$ and $2H_2@C_{60}$ of I_h, D_{5d} and C_{2h} symmetry, respectively, were considered in this work (Figure 1). All MP2 calculations were performed with the GAUSSIAN 09 program package [29], whereas DF-LMP2 ones were performed with the MOLPRO program package [30], under the frozen-core approximation in all cases. MP2 geometry optimizations using analytical gradients were carried out with Pople-style split valence basis sets ranging from 3-21G [31] to 6-311G(d,p) [32], as well as with the correlation-consistent polarized valence cc-pVDZ and cc-pVTZ basis sets of Dunning [33], using default GAUSSIAN 09 convergence criteria. Unfortunately, calculations with the larger aug-cc-pVTZ basis set were not possible because of a linear dependency problem. The DF-LMP2 calculations were performed with the cc-pVDZ and cc-pVTZ basis sets [33]. The density-fitting Hartree–Fock (DF-HF) reference wave functions were first obtained with the corresponding JKFIT basis sets [34] and a convergence threshold for density matrix elements of 10^{-14}, while the density fitting in the subsequent MP2 calculations was taken into account through the corresponding MP2FIT basis sets [35]. The orbital localization in the local correlation approach was carried out using the Pipek–Mezey procedure [36]. Standard orbital domains were formed on the basis of the Boughton and Pulay selection criterion of 0.98 [37]. Analytical gradients [38] were employed for the DF-LMP2 geometry optimizations using a maximum gradient component of 10^{-5} a.u.

The complexation energy of the $nH_2@C_{60}$ ($n = 1, 2$) systems is determined as the difference between the energy of the complex and that of the separate nH_2 and C_{60} molecules, as

$$\Delta E = E(nH_2@C_{60}) - [E(C_{60}) + n(H_2)],$$

where $E(nH_2@C_{60})$, $E(C_{60})$ and $E(H_2)$ correspond to the total energies of the fully-optimized complex, fullerene C_{60} and H_2 molecule, respectively. The basis set superposition error (BSSE) was calculated with the standard counterpoise method of Boys and Bernardi [22].

The infrared spectral signature of the encapsulated H_2 molecule was also evaluated for connection with experimental data [39–41]. A complete evaluation of the force constant matrix, and thus a full vibrational analysis, is not practical for systems as large as $nH_2@C_{60}$

at the (DF-L)MP2 level of theory. Therefore, we estimated the H—H force constant, i.e. the second derivative of the energy with respect to position, numerically by three-point central finite differences of the energy. A symmetric displacement of ±0.005 Å was used for the H atoms of the H_2 molecule. The corresponding H_2 harmonic vibrational frequency – and the frequency shift relative to that of free H_2, was then evaluated with this estimate of the force constant. The frequencies obtained were further scaled using the recommended scaling factors of 0.956 for DF-LMP2/cc-pVTZ and 0.955 for MP2/cc-pVTZ [42].

3. Results and discussion

The equilibrium geometry parameters of fullerene C_{60} and its endohedral complexes with one and two hydrogen molecules obtained with different MP2 model chemistries (calculated in this work and reported in the literature) and from experiment are listed in Table 1, the harmonic H—H vibrational frequencies of H_2 in the free and encapsulated states are collected in Table 2, while the complexation energies of $H_2@C_{60}$ and $2H_2@C_{60}$ are given in Tables 3 and 4, respectively.

As can be seen from the data in Table 1, upon increase of basis set size from double to triple-zeta quality, the MP2 optimized bond lengths of C_{60} become shorter by up to 1%, with the length of the formally double C=C bond approaching (within 0.003 Å) the experimental X-ray value reported by Hedberg et al. [43]. However, the formally single C—C bond length is underestimated with a triple-zeta basis set by 1%, compared to the experimental value of 1.458 Å reported by Hedberg et al. [43], but the deviation from experimental data is less pronounced when compared to other experimental data (cf. Table 1). Further extension of the basis set from triple (cc-pVTZ) to quadruple zeta (cc-pVQZ) was shown to shorten both C—C and C=C bond lengths of C_{60} by only 0.002 Å [44], and therefore the C_{60} geometry optimization can be considered converged with MP2/cc-pVTZ. The optimized DF-LMP2 bond lengths of C_{60} coincide with their MP2 counterparts for hexagon–hexagon bonds, but they are slightly underestimated in the case of pentagon-hexagon bonds with respect to MP2 (by only 0.003–0.004 Å).

The data in Table 1 shows that the $H_2@C_{60}$ complex is characterized by the same C—C bond lengths as those of a free C_{60} cage optimized with the same model chemistry. However, in this complex, the H—H bond length is usually larger by 0.007–0.010 Å than that of free H_2. One would thus expect that the vibrational frequency
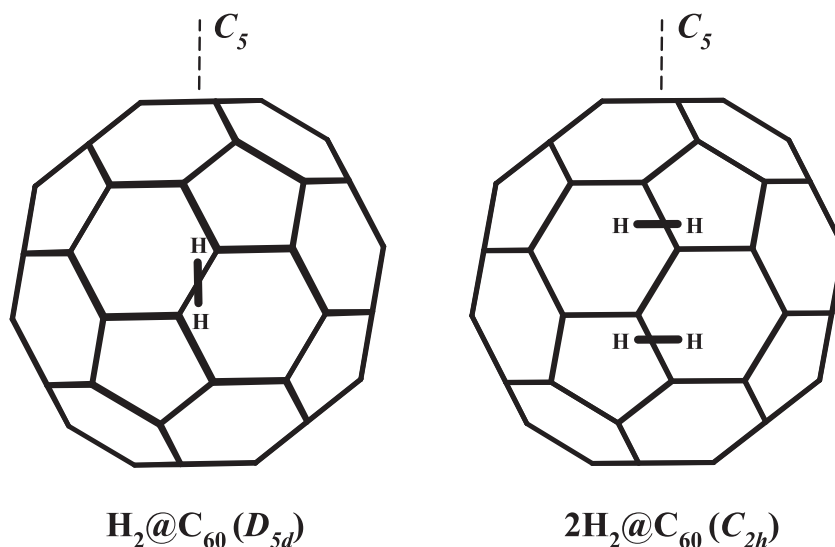

Figure 1. Structures of the $H_2@C_{60}$ and $2H_2@C_{60}$ complexes considered in this work. The location of the C_5 axis and the orientation of the H_2 molecules are also shown.

Table 1
Calculated and available experimental equilibrium geometry parameters of C_{60}, $H_2@C_{60}$ and $2H_2@C_{60}$.[a]

	R (5–6)	R (6–6)	R (H–H)[b]	Refs.
C_{60}				
MP2/DZ	1.470	1.407	–	[46]
MP2/DZP	1.451	1.412	–	[46]
MP2/TZP	1.446	1.406	–	[46]
MP2/cc-pVDZ	1.454	1.416	–	This work
MP2/cc-pVTZ	1.443	1.404	–	This work, [44]
MP2/cc-pVQZ	1.441	1.402	–	[44]
DF-LMP2/cc-pVDZ	1.458	1.416	–	This work
DF-LMP2/cc-pVTZ	1.446	1.404	–	This work
Exp.[c]	1.45 ± 0.015	1.40 ± 0.015	–	[47]
Exp.[d]	1.432 (5)	1.388 (9)	–	[48]
Exp.[e]	1.458 (6)	1.401 (10)	–	[43]
Exp.[f]	1.455 (12)	1.391 (18)	–	[49]
$H_2@C_{60}$				
MP2/cc-pVDZ	1.454	1.416	0.761	This work
MP2/cc-pVTZ	1.443	1.404	0.747	This work
DF-LMP2/cc-pVDZ	1.458	1.416	0.759	This work
DF-LMP2/cc-pVTZ	1.446	1.404	0.745	This work
$2H_2@C_{60}$				
MP2/cc-pVDZ	1.455	1.417	0.752	This work
MP2/cc-pVTZ	1.443	1.405	0.739	This work
DF-LMP2/cc-pVDZ	1.459	1.417	0.749	This work
DF-LMP2/cc-pVTZ	1.447	1.405	0.737	This work

[a] R (5–6), R (6–6) and R (H–H) represent the carbon–carbon bond lengths in fullerene that join five and six-membered rings, six-membered rings, and the bond length of the encapsulated H_2 molecule, respectively. All values are in Å.

[b] The H–H bond length of free H_2 optimized at the (DF-L) MP2 level of theory is 0.754 and 0.737 Å with the cc-pVDZ and cc-pVTZ basis sets, respectively.

[c] As determined by solid-state ^{13}C NMR.

[d] From X-ray data for the osmylated C_{60} derivative, $C_{60}(OsO_4)(4\text{-}tert\text{-butyl-pyridine})_2$.

[e] Deduced from gas-phase electron diffraction measurements of C_{60}.

[f] From neutron powder diffraction measurements of C_{60} at 5 K.

associated with the H—H vibrational stretching mode would undergo a red shift (i.e., a shift to smaller wavenumbers) in the $H_2@C_{60}$ complex, relative to that of the free H_2 molecule. Indeed, as evident from the data in Table 2, both DF-LMP2/cc-pVTZ and MP2/cc-pVTZ predict a red shift of the H_2 vibrational frequency by about 120–160 cm^{-1} for this system. This finding is consistent with the recent experimental observation of red shifts of 23 cm^{-1} in an open-cage fullerene [39] by Raman spectroscopy, as well as 90 cm^{-1} [40] and 98.8 cm^{-1} [41] by infrared spectroscopy, for the H—H vibrational stretching frequency of the complexed H_2 molecule in the endohedral $H_2@C_{60}$. It should be noted that lower-level quantum chemistry approaches based on Hartree–Fock theory [45] or on DFT [26] are, in general, not able to reproduce this effect, as it originates from the numerous, weak, attractive van der Waals interactions between the carbon atoms of the fullerene cages and

the hydrogen atoms of the H_2 molecule, which lead to the H—H bond lengthening. For the same reason, a similar red shift (but less pronounced – about 60 cm^{-1}) was also observed for exohedrally-bound H_2 molecules in C_{60} crystals [41].

In contrast, the $2H_2@C_{60}$ complex is characterized by a slight elongation of the carbon–carbon bonds in the cage, while the H—H bond lengths of the H_2 molecules inside remain unchanged with DF-LMP2/cc-pVTZ or marginally larger with MP2/cc-pVTZ, relative to that of free H_2 (cf. Table 1). Therefore, for $2H_2@C_{60}$, one would expect a blue shift (i.e., a shift to larger wavenumbers) in the infrared spectral region of the normal modes associated with C—C bond stretching in C_{60}, and an H—H vibrational signature similar to that of the uncomplexed H_2 molecule. In fact, the calculated H—H vibrational frequencies for the $2H_2@C_{60}$ complex are predicted to be slightly blue-shifted ($\sim$40 cm^{-1}) with DF-LMP2/cc-pVTZ or red-shifted ($\sim$60 cm^{-1}) with MP2/cc-pVTZ (cf. Table 2). The latter is most likely a result of the overestimated binding between the guest and the host with MP2, as reflected in complexation energies that are too large in magnitude compared to DF-LMP2 (see also the discussion below). We note, however, that the experimental validation of these trends will be rather difficult to achieve because of the thermodynamic instability of this complex, as now discussed.

All MP2 approaches confirm that the $H_2@C_{60}$ complex is thermodynamically stable (cf. Table 3). Calculations employing small double-zeta-quality basis sets usually suffer from significant BSSE (about 2 kcal/mol), and as a result, accounting for BSSE significantly reduces the magnitude of the complexation energies of $H_2@C_{60}$. In some cases, even triple-zeta Pople-style basis sets may lead to a BSSE in the range 2.6–3.7 kcal/mol. When employing a triple-zeta cc-pVTZ basis set in conjunction with MP2, a BSSE-corrected complexation energy value of −6.4 kcal/mol is obtained – in agreement with the value of −7.0 ± 1.0 kcal/mol estimated by Kruse and Grimme [25], based on the spin-component-scaled (SCS)-MP2 and MP2.5 complete-basis-set (CBS) extrapolation. This value is slightly larger in magnitude than the symmetry-adapted perturbation theory (SAPT) value of −4.6 kcal/mol reported by Korona et al. [3], and may reflect the degree of uncertainty in the calculated complexation energies caused by a slight overestimation of MP2 binding energies for weakly bound systems in general, and the moderate size of the basis set employed by Korona et al. [3]. The DF-LMP2 complexation energies of $H_2@C_{60}$ agree within 0.7–0.8 kcal/mol with their MP2 counterparts, but a significant advantage of the DF-LMP2 approach is that the BSSE becomes insignificant with the triple-zeta cc-pVTZ basis set (and presumably larger basis sets), making the additional counterpoise-correction calculations unnecessary. The DF-LMP2/cc-pVTZ complexation energy value of −5.6 kcal/mol lies right in between those reported by Kruse and Grimme [25] and by Korona et al. [3].

Table 2
Harmonic H–H vibrational frequencies for H_2, $H_2@C_{60}$ and $2H_2@C_{60}$ and corresponding shifts Δv upon complexation.[a]

	H_2	$H_2@C_{60}$	$2H_2@C_{60}$	$\Delta v(H_2@C_{60})$	$\Delta v(2H_2@C_{60})$
DF-LMP2/cc-pVTZ unscaled	4526	4401	4566	125	−40
DF-LMP2/cc-pVTZ scaled[b]	4327	4207	4365	120	−38
MP2/cc-pVTZ unscaled	4525	4365	4463	160	62
MP2/cc-pVTZ scaled[c]	4321	4169	4262	152	59
IR Spectroscopy[d]	4161.2	4071.4	–	89.8	–
IR Spectroscopy[e]	4161.2	4062.4	–	98.8	–
Raman Spectroscopy[f]	4158	4135	–	23	–

[a] $\Delta v = v(H_2) - v(nH_2@C_{60})$. Positive values indicate a red shift, negative values a blue shift.

[b] The scaling factor is 0.956 [42].

[c] The scaling factor is 0.955 [42].

[d] Measured at 6 K. From Ref. [40].

[e] Measured at 6 K, and including a correction for the different zero-point energies of the $v = 0$ and 1 states; see Ref. [41].

[f] Measured for the $H_2@$open-cage fullerene at 20 K; see Ref. [39].

Table 3
Calculated complexation energies of $H_2@C_{60}$.[a]

	ΔE	BSSE	ΔE + BSSE	Refs.
MP2/3-21G	−2.5	2.3	−0.2	This work
MP2/6-31G//HF/6-31G	−2.1	–	–	[27]
MP2/6-31G*	−2.9	1.7	−1.2	This work
MP2/6-31G**//exp.geom.[b]	−4.0	1.6	−2.4	[28]
MP2/cc-pVDZ	−5.8	2.2	−3.6	This work
MP2/cc-pVDZ//B3LYP/6-31G**	−5.6	2.3	−3.3	[26]
MP2/6-311G(d,p)	−7.3	3.2	−4.1	This work
MP2/6-311G(2d,2p)//exp.geom.[b]	−8.6	2.6	−6.0	[28]
MP2/(d,p)-6-311G(d,p)[c]//exp.geom.[b]	−10.6	3.7	−6.9	[28]
MP2/TZVPP//exp.geom.[b]	−7.3	–	–	[3]
MP2/cc-pVTZ	−7.7	1.3	−6.4	This work
DF-LMP2/cc-pVDZ	−3.5	0.6	−2.9	This work
DF-LMP2/cc-pVTZ	−5.7	0.1	−5.6	This work
DF-MP2/aug-def2-TZVPP//PBE/SVP	−9.5	–	–	[25]
DF-MP2/TQZP//PBE-D/def2-TZVPP	−9.6	1.0	−8.6	[25]

[a] All values in kcal/mol.
[b] Single-point energy calculation based on the experimental geometry of C_{60} [43].
[c] See Ref. [50] for details regarding the augmented (d,p)-6-311G(d,p) basis set.

Table 4
Calculated complexation energies of $2H_2@C_{60}$.[a]

	ΔE	BSSE	ΔE + BSSE	Refs.
MP2/cc-pVDZ	0.9	7.1	8.0	This work
MP2/cc-pVDZ//B3LYP/6-31G**	0.9	7.0	7.9	[26]
MP2/TZVPP//exp.geom.[b]	−0.98, −1.05[c]	–	–	[3]
MP2/cc-pVTZ	−2.8	3.7	0.9	This work
DF-LMP2/cc-pVDZ	7.8	2.7	10.5	This work
DF-LMP2/cc-pVTZ	2.4	0.6	3.0	This work
DF-MP2/aug-def2-TZVPP//PBE/SVP	−6.7	–	–	[25]
DF-MP2/TQZP//PBE-D/def2-TZVPP	−6.7	2.4	−4.3	[25]

[a] Calculated for the complex with a parallel arrangement of the H_2 molecules with respect to a pentagon ring of C_{60} (cf. Figure 1). All values in kcal/mol.
[b] Single-point energy calculation based on the experimental geometry of C_{60} [43].
[c] Determined for the crossed XP and XH structures, respectively. For notation details, see Ref. [3].

Based on the van der Waals radii of hydrogen and carbon atoms, it can be easily shown [1–3] that the insertion of two H_2 molecules into the C_{60} cage should not be a thermodynamically favored process. This is reflected in the slight cage expansion of C_{60} upon insertion of two H_2 molecules discussed above. In line with these expectations, MP2 calculations with a small double-zeta cc-pVDZ basis set results in a positive complexation energy (and incidentally a large BSSE) for $2H_2@C_{60}$ (cf. Table 4). However, with triple-zeta and larger basis sets, DF-MP2 (as well as MP2 without BSSE correction) tends to overestimate the binding in this complex, resulting in a complexation energy as large as −4.3 kcal/mol in magnitude, the latter being obtained with DF-MP2/TQZP [25]. This discrepancy can be remedied, on the one hand, by the use of the SCS-MP2 approach, leading to a final CBS-extrapolated complexation energy of 2.0–2.3 kcal/mol [25]. On the other hand, DF-LMP2 together with the triple-zeta cc-pVTZ basis set yields uncorrected and BSSE-corrected complexation energies of 2.4 and 3.0 kcal/mol, respectively. These values agree not only with previously mentioned SCS-MP2-CBS estimates [25], but they also lie close to the DFT-SAPT value of 5.9 kcal/mol (for the 'crossed' configuration of H_2 molecules inside the cage) [3]. We note that geometry relaxation of the hydrogen molecules inside the cage (leading to the 'crossed' configuration) stabilizes the complex by only 0.1 kcal/mol, relative to the C_{2h} symmetry-restrained configuration, according to DF-LMP2/cc-pVTZ. This energy difference is within the typical error bars of the calculations and it is too small to unambiguously assert which conformation is the true global minimum-energy structure. In summary, DF-LMP2 provides correct

energetic characteristics of the $nH_2@C_{60}$ complexes when used in conjunction with basis sets of at least triple-zeta quality.

4. Conclusions

Density-fitting local second-order Møller–Plesset (DF-LMP2) theory yields a correct description of the geometries and complexation energies of the $nH_2@C_{60}$ (n = 1, 2) complexes in comparison to much more computationally expensive conventional (spin-component-scaled) MP2 and DFT-SAPT approaches. After full DF-LMP2 geometry optimization, only the $H_2@C_{60}$ complex is found to be thermodynamically stable. With the cc-pVTZ basis set, the DF-LMP2 complexation energies are equal to −5.6 and +3.0 kcal/mol, for one and two inserted H_2 molecules, respectively. Conventional MP2 calculations tend to overestimate the stabilization in $H_2@C_{60}$ and even predict erroneous stabilization in $2H_2@C_{60}$. A significant advantage of DF-LMP2 is that the usual counterpoise-correction calculation in the determination of complexation energies becomes unnecessary for triple-zeta and presumably larger basis sets. DF-LMP2 also correctly predicts a slight elongation of the H—H bond and, consequently a red shift of the H—H vibrational stretching frequency in the $H_2@C_{60}$ complex relative to the uncomplexed H_2 molecule, in excellent agreement with recent experimental findings. In contrast, for the thermodynamically unstable $2H_2@C_{60}$ complex, one would expect the same H_2 infrared spectral signature as for free H_2 (as the H—H bond lengths are essentially the same in the complexed and uncomplexed cases), but a blue shift for the vibrational modes associated with the C—C bond stretching of the C_{60} cage resulting from a slight expansion of the cage upon complexation. The reported calculations constitute the highest level of quantum chemistry at which the geometries of the $nH_2@C_{60}$ (n = 1, 2) complexes have ever been characterized.

Acknowledgements

References

[1] G. Dolgonos, J. Mol. Struct.-Theochem. 732 (2005) 239.
[2] G. Dolgonos, Carbon 46 (2008) 704.
[3] T. Korona, A. Hesselmann, H. Dodziuk, J. Chem. Theory Comput. 5 (2009) 1585.
[4] T. Janowski, P. Pulay, Chem. Phys. Lett. 447 (2007) 27.
[5] S. Grimme, J. Antony, T. Schwabe, C. Mück-Lichtenfeld, Org. Biomol. Chem. 5 (2007) 741.
[6] P. Hobza, K. Müller-Dethlefs, Non-covalent Interactions. Theory and Experiment, Royal Society of Chemistry, Cambridge, 2010.
[7] W. Kohn, Y. Meir, D.E. Makarov, Phys. Rev. Lett. 80 (1998) 4153.
[8] J.M. Tao, J.P. Perdew, V.N. Staroverov, G.E. Scuseria, Phys. Rev. Lett. 91 (2003) 146401.
[9] Y. Zhao, D.G. Truhlar, J. Phys. Chem. A 108 (2004) 6908.
[10] Y. Zhao, D.G. Truhlar, J. Chem. Phys. 125 (2006) 194101.
[11] Y. Zhao, D.G. Truhlar, Acc. Chem. Res. 41 (2008) 157.
[12] S. Grimme, J. Chem. Phys. 124 (2006) 034108.
[13] L.A. Burns, A. Vázquez-Mayagoitia, B.G. Sumpter, C.D. Sherrill, J. Chem. Phys. 134 (2011) 084107.
[14] S. Grimme, J. Comput. Chem. 25 (2004) 1463.
[15] S. Grimme, J. Antony, S. Ehrlich, H. Krieg, J. Chem. Phys. 132 (2010) 154104.
[16] C.D. Sherrill, J. Chem. Phys. 132 (2010) 110902.
[17] P. Pulay, Chem. Phys. Lett. 100 (1983) 151.
[18] S. Saebø, P. Pulay, Chem. Phys. Lett. 113 (1985) 13.
[19] S. Saebø, P. Pulay, J. Chem. Phys. 115 (2001) 3975.
[20] O. Vahtras, J. Almlöf, M.W. Feyereisen, Chem. Phys. Lett. 213 (1993) 514.
[21] H.J. Werner, F.R. Manby, P.J. Knowles, J. Chem. Phys. 118 (2003) 8149.
[22] S.F. Boys, F. Bernardi, Mol. Phys. 19 (1970) 553.
[23] C. Møller, M.S. Plesset, Phys. Rev. 46 (1934) 618.
[24] J.G. Hill, J.A. Platts, H.J. Werner, Phys. Chem. Chem. Phys. 8 (2006) 4072.

[25] H. Kruse, S. Grimme, J. Phys. Chem. C 113 (2009) 17006.
[26] T.B. Lee, M.L. McKee, J. Am. Chem. Soc. 130 (2008) 17610.
[27] C.N. Ramachandran, D. Roy, N. Sathyamurthy, Chem. Phys. Lett. 461 (2008) 87.
[28] Z. Slanina, P. Pulay, S. Nagase, J. Chem. Theory Comput. 2 (2006) 782.
[29] M.J. Frisch, G.W. Trucks, H.B. Schlegel, G.E. Scuseria, M.A. Robb, et al., GAUSSIAN 09, Revision A.02, Gaussian Inc., Wallingford, CT, 2009.
[30] H.-J. Werner, P.J. Knowles, R. Lindh, F.R. Manby, M. Schütz, et al., MOLPRO, version 2006.1, a package of ab initio programs. See http://www.molpro.net.
[31] J.S. Binkley, J.A. Pople, W.J. Hehre, J. Am. Chem. Soc. 102 (1980) 939.
[32] R. Krishnan, J.S. Binkley, R. Seeger, J.A. Pople, J. Chem. Phys. 72 (1980) 650.
[33] T.H. Dunning Jr, J. Chem. Phys. 90 (1989) 1007.
[34] F. Weigend, Phys. Chem. Chem. Phys. 4 (2002) 4285.
[35] F. Weigend, A. Köhn, C. Hättig, J. Chem. Phys. 116 (2002) 3175.
[36] J. Pipek, P.G. Mezey, J. Chem. Phys. 90 (1989) 4916.
[37] J.W. Boughton, P. Pulay, J. Comput. Chem. 14 (1993) 736.
[38] M. Schütz, H.J. Werner, R. Lindh, F.R. Manby, J. Chem. Phys. 121 (2004) 737.
[39] P.M. Rafailov, C. Thomsen, A. Bassil, K. Komatsu, W. Bacsa, Phys. Status Solidi B 242 (2005) R106.
[40] S. Mamone et al., J. Chem. Phys. 130 (2009) 081103.
[41] M. Ge et al., J. Chem. Phys. 134 (2011) 054507.
[42] T. Hrenar, G. Rauhut, H.J. Werner, J. Phys. Chem. A 110 (2006) 2060.
[43] K. Hedberg, L. Hedberg, D.S. Bethune, C.A. Brown, H.C. Dorn, R.D. Johnson, M. de Vries, Science 254 (1991) 410.
[44] C. Hättig, A. Hellweg, A. Köhn, Phys. Chem. Chem. Phys. 8 (2006) 1159.
[45] J. Cioslowski, J. Am. Chem. Soc. 113 (1991) 4139.
[46] M. Häser, J. Almlöf, G.E. Scuseria, Chem. Phys. Lett. 181 (1991) 497.
[47] C.S. Yannoni, P.P. Bernier, D.S. Bethune, G. Meijer, J.R. Salem, J. Am. Chem. Soc. 113 (1991) 3190.
[48] J.M. Hawkins, A. Meyer, T.A. Lewis, S. Loren, F.J. Hollander, Science 252 (1991) 312.
[49] W.I.F. David et al., Nature 353 (1991) 147.
[50] S. Tsuzuki, T. Uchimaru, M. Mikami, K. Tanabe, J. Phys. Chem. A 102 (1998) 2091.